

Contribution of crystal-impeller and crystal-crystal collisions to secondary nucleation

A. Imran*, E. Wolf, H.J.M. Kramer, P.J. Jansens

Process & Energy Department, Delft University of Technology, Leeghwaterstraat 44, 2628 CA Delft, The Netherlands

Abstract

A secondary nucleation model mainly based on the findings of Ottens (1973) and Evans (1974) considering both crystal-impeller collisions and crystal-crystal collisions was investigated using experimental data obtained from two crystallizers, a 22-liter Draft Tube (DT) crystallizer and an 1100-liter Draft Tube Baffled (DTB) crystallizer, which are both operated continuously in an evaporative mode for the crystallization of ammonium sulfate. Since the two crystallizer types differ in scale and configuration, not only the effect of the impeller frequency but also the effect of scale on the crystal size distribution (CSD) could be investigated. The CSD-prediction obtained using dynamic process simulations is consistent with the measured data for all investigated experiments. Not only the changes in the CSD due to different impeller frequencies, but also the changes due to scale and configuration are well described and model is able to capture the sustained cyclic behavior in DTB crystallizer. It was found that three model parameters i.e. the number of nuclei per unit energy, the lower bound of integration for the crystal-impeller and for the crystal-crystal collisions are a function of the impeller frequency and should therefore be altered accordingly. Therefore the predictive capability of this model is limited. In the 22-liter DT-crystallizer crystal-impeller collisions are dominating while crystal-crystal collisions are of less importance. Nevertheless, crystal-crystal collisions cannot be neglected and are especially pronounced at low impeller frequencies. In the 1100-liter DTB-crystallizer the term of the secondary nucleation rate equation describing crystal-crystal collisions is more important. But this effect cannot be attributed only to crystal-crystal collisions. Since the supersaturation in the DTB-crystallizer is higher, and the circulation time is larger compared to the DT-crystallizer, it is expected that also the surface breeding in combination with a fluid shear mechanism is responsible for the production of secondary nuclei.

Keywords: crystal-impeller collisions, crystal-crystal collisions, secondary nucleation, industrial crystallization

1. Introduction

Crystallization is a chemical process that can be divided into a number of sub-processes like primary and secondary nucleation, crystal growth and hydrodynamic and mechanical processes. Since crystallization is a particulate process a population balance is required in addition to the usual mass and energy balances. The complexity in describing a crystallization process is that the different sub-processes cannot be studied separately since they are coupled and therefore influence each other. In many crystallization processes product purity and Crystal Size Distribution (CSD) are of prime importance, especially when considering the ever-increasing demands of the customers. Furthermore, crystals produced through a crystallization process have a decisive influence on the downstream processing (filterability, washability, dryability etc.) and therefore the CSD should be predictable, reproducible in each operation and as regular as possible (Ma et al., 2002).

It is now well-established that secondary nucleation plays an important role in determining the product crystal size distribution in most forms of industrial suspension crystallizer. Possible mechanisms of secondary nucleation are numerous though one which is widely reported concerns contact or collision breeding which occurs as a result of impacts of crystals with each other and/or with other solid objects, e.g. vessel walls or a rotating impeller. The most classical expression for the secondary nucleation rate in a suspension of growing crystals is the empirical power law that contains three experimentally accessible parameters. These parameters give a description of the state of the fluid phase in the crystallizer (for example the relative supersaturation), the CSD (moment of distribution, crystal mass) and the mechanical agitation in the crystallizer (stirrer speed, mechanical dissipation). Although the classical power law can be used to describe the steady-state CSD, it fails to describe the dynamics in a crystallization process.

Ottens et al. (1972) was the first to develop a mechanistic description of the mechanical interaction of the crystals with the crystallizer hardware in which the nucleation rate of the crystals is assumed to be proportional to the product of collision energy and frequency of collision. Moreover a lower bound of integration was introduced into the distribution in order to account for the phenomenon that larger crystals are more prone to attrition. Evans et al. (1974) used the same basic approach as Ottens, but besides crystal-impeller collisions due to bulk flow and crystal-crystal collisions due to turbulence, they distinguished additional collision mechanisms like crystal impeller collisions due to turbulence, and crystal-crystal collisions induced by gravity.

Another approach towards the simulation of the dynamics of the crystallization process was introduced by Ó Meadhra (1995), who determined an attrition function for the parent crystals under growing conditions. Gahn and Mersmann (1999) developed a more fundamental approach of the generation of secondary nuclei based on material properties and physical concepts. An important assumption of this model is that in particular the crystal corners contribute to the generation of attrition

fragments since they possess higher local stresses. Moreover it was assumed that the crystals have sufficient time to grow between two subsequent collisions, thereby redeveloping their corners.

Although these models can be used to describe the steady-state CSD, they fail to describe the dynamics in a crystallization process and to predict the nucleation behavior for different process conditions. In present contribution, a secondary nucleation model is developed based on the work of Ottens (1973) and Evans (1974), which considers both crystal-impeller and crystal-crystal collisions. The aim of the research is develop a model, which is capable to describe the dynamic behavior of the crystallization process and can predict the nucleation behavior, not only for different impeller frequencies, but also for different scales and configuration.

2. The secondary nucleation model

According to Evans et al. (1974), secondary nucleation can be considered as a two step process. In the first step, a new nucleus is originated on the surface of a stable parent crystal. A consequent second step is the displacement of this nucleus from the surface into the bulk by a removal mechanism. Two mechanisms of removal are considered: collisions of the crystal with the crystallizer (impeller, baffles and wall), and the collisions of the crystals with one another. The secondary nucleation rate is proportional to the product of origination and removal, where the origination of nuclei is described by the number of nuclei per unit energy, Ω , and the removal process by the rate of energy transfer, $(E_j)^{4,5}$. Consequently, the nucleation rate attributable to different removal mechanisms is additive:

$$J_i = \Omega \cdot E_j \quad (0.1)$$

$$J_t = \sum J_j = \Omega \cdot \sum E_j \quad (0.2)$$

where (J_t) is the overall nucleation rate with two or more mechanisms of removal is the linear sum of the actual nucleation rate attributable to each mechanism of removal (J_j) , and j indicates the type of removal process (i.e. $c - i$ for crystal-impeller and $c - c$ for crystal-crystal)

Evans proposes three idealized mechanisms of removal: Collisions of crystals with the crystallizer (impeller, baffles, wall), collisions between crystals driven by turbulent eddy motion, and collision between crystals as of consequence of differences in their terminal velocities (gravitational forces)⁵. In present approach, the latter term is not taken into account due to the assumption that gravitational forces can be neglected due to the high circulation velocities of the fluid in the crystallizer. Therefore in present model only the collisions with the impeller and with other crystals are considered as removal mechanism.

The secondary nucleation models for both crystal-impeller and crystal-crystal collisions are given by Ottens et al. (1972). These models are based on experiments by Clontz and McCabe (1971). In these experiments they allowed a single $\text{MgSO}_4 \cdot 7\text{H}_2\text{O}$ crystal to collide, in a well defined way, with a metal rod or another single crystal. Using the obtained experimental observations, Ottens derived the following equation for the contribution to the total net nucleation rate of $n_L dL$ crystals between size L and $L + dL$:

$$dJ = k (\sigma)^g \omega_L E_L n_L dL \quad (0.3)$$

Where k is the empirical nucleation constant, σ is the supersaturation, g is an empirical growth order, ω_L is the collision frequency of crystals between size L and $L + dL$, ω_L and E_L are the collision frequency and the impact energy at the surface of a crystal between size L and $L + dL$, n_L is the number density. To find the total nucleation rate over the whole size interval, Eq. (0.3) must be integrated:

$$J = \int_0^{\infty} dJ = \underbrace{k_n}_{\Omega} \cdot \int_0^{\infty} \underbrace{\omega_L E_L n_L}_{E_j} dL \quad (0.4)$$

Where k_n is the constant that takes into account the σ as well. From Eq. (2.1) it follows that the number of nuclei generated per unit energy (Ω) is equal to k_n , while the rate of energy transfer corresponds to the term over which the integral is taken.

Eq. (2.4) is integrated over the whole size range, which assumes that every particle in every size range contributes in collisions with either the impeller or other crystals. In reality particles with small inertia (low mass and/or velocity) will not or hardly contribute to collisions with the impeller or other crystals due to insignificant hydrodynamic and mechanical forces (Bermingham, 2003). The influence of these small crystals to the secondary nucleation rate is therefore negligible. Therefore a lower bound of integration is introduced into Eq. (2.4):

$$J = \int_{L_j}^{\infty} dJ = \underbrace{k_n}_{\Omega} \cdot \int_{L_j}^{\infty} \underbrace{\omega_L E_L n_L}_{E_j} dL \quad (0.5)$$

The value of L_j will differ for the different kinds of collisions, and should be determined for crystal-crystal collisions and crystal-impeller collisions separately. These bounds indicate that crystals with a size smaller than this lower bound are excluded from the distribution.

Nucleation attributable to crystal-impeller collisions

For the case of crystal-impeller collisions, Ottens assumed that the collision frequency, ω_L , of a crystal with the impeller is size-independent and proportional to the circulation time, tc , which is defined as the time interval between two subsequent passages of a crystal through the impeller area.

$$\omega_L \propto \frac{1}{t_c} = \frac{\varphi_{vp}}{V_c} = \frac{KND^3}{V_c}, \quad (0.6)$$

where φ_{vp} is the pumping capacity of the impeller, V_c is the total volume of the crystallizer, K is the impeller discharge coefficient, N is the impeller speed, and D is the impeller diameter. Assuming that only the collisions with the tip of the impeller blade are relevant, the impact energy E_L , is proportional to the mass, m_L , and the square of the tip speed of the impeller v_t :

$$E_L \propto m_L v_t^2 \propto m_L (ND)^2 \quad (0.7)$$

Substitution of equation Eq. (2.6) and Eq. (2.7) in equation Eq. (2.5) yields for crystal-impeller collisions:

$$J_{c-i} \propto k_{c-i} \cdot \int_{L_{c-i}}^{\infty} \frac{KN^3 D^5}{V_c} \cdot m_L \cdot n_L \cdot dL \quad (0.8)$$

The group $(N^3 D^5)/V_c$ can be correlated to dissipated power by the impeller per unit mass of suspension, ε , according to:

$$\varepsilon = \frac{P_0 N^3 D^5}{V_c}, \quad (0.9)$$

where P_0 is the dimensionless impeller power number. Using the fact that $m_L = \rho_c k_v L^3$, Eq. (2.8) results in:

$$J_{c-i} \propto k_{c-i} \cdot \frac{K}{P_0} \cdot k_v \cdot \rho_c \cdot \varepsilon \int_{L_{c-iL}}^{\infty} L^3 \cdot n_L \cdot dL \quad (0.10)$$

Nucleation attributable to crystal-crystal collisions

In comparison with crystal-impeller collisions the impact energy is much less in the case of crystal-crystal collisions, but the total collision frequency may be so high, that the net effect on nucleation cannot be neglected. According to Evans, it is assumed that crystals driven by turbulence will follow any eddy of size greater than their size but will not follow an eddy of smaller size. Thus, smaller crystals will follow a greater range of eddy sizes and collide with larger crystals. A consequence of the basic hypothesis is that the crystals will have motion relative to each other and collide only if their crystals are of different size.

To determine the collision frequency it is assumed that all crystals are spherical and equal the mean crystal size, \bar{L} . To calculate the mean collision frequency $\bar{\omega}$, Ottens proposed that the trajectory of a crystal relative to the solution per second is equal to v_{rel} and corresponds to a flow of solution of volume V_l :

$$V_l = \frac{1}{4} \pi \bar{L}^2 v_{rel} \quad (0.11)$$

In other words, V_l equals the volume displaced by the particle per second. If the total number of crystals per unit volume is μ_0 , the crystals that are available in this displaced volume, equals $\mu_0 V_l$. This yields for the mean collision frequency:

$$\bar{\omega} = \frac{1}{4} \mu_0 \pi \bar{L}^2 v_{rel} \quad (0.12)$$

The relative velocity v_{rel} of a particle with size \bar{L} can be calculated with the theory of local isotropic turbulence. Levich calculates the motion of a particle in a turbulent field by means of a particle force balance:

$$v_{rel} \propto \left(\frac{\rho_s - \rho_l}{\rho_s} \right)^{1/2} \left(\frac{\rho_s}{\rho_l} \right)^{1/3} \left(\frac{1}{C_D} \right)^{1/3} \epsilon^{1/3} \bar{L}^{1/3} \quad (0.13)$$

where C_D is the drag coefficient. Ottens assumed that the drag coefficient is a constant. This is true only for Reynolds numbers in a range of $1 \cdot 10^3$ to $2 \cdot 10^5$, which is not applicable here. Evans states that for most cases of practical interest, the Reynolds number is in the intermediate regime, $2 \leq Re_p \leq 500$, where the drag coefficient is inversely proportional to the 0.6 power of the Reynolds number:

$$C_D = \frac{18.5}{Re_p^{0.6}} \propto \left(\frac{\eta}{\rho v_{rel} \bar{L}} \right)^{0.6} \quad (0.14)$$

Solving Eq. (0.14) & Eq. (0.13) for the relative velocity, v_{rel} can be approximated as:

$$v_{rel} \sim \epsilon^{5/12} \cdot \bar{L}^{2/3} \quad (0.15)$$

The impact energy \bar{E}_L is assumed to be proportional to the kinetic energy of the moving crystal:

$$\bar{E}_L \propto E_{kin} = \frac{1}{2} m_L v_{rel}^2 \quad (0.16)$$

When substituting the equations for the mean collision frequency and impact energy in Eq. (2.5), the secondary nucleation rate for crystal-crystal collisions is:

$$J_{c-c} \propto k_{c-c} \cdot \pi k_v \rho_c \varepsilon^{5/4} \bar{L}^{-7} \mu_0^2 \quad (0.17)$$

The weight fraction of crystals per unit volume of liquor, ϕ_c , can be expressed as:

$$\phi_c = \frac{k_v \rho_c \pi \bar{L}^{-3} \mu_0}{6 \rho_{sl}} \quad (0.18)$$

where the density of de slurry is denoted as ρ_{sl} . this yields for the equation that describes crystal-crystal collisions:

$$J_{c-c} \propto k_{c-c} \rho_{sl}^3 \varepsilon^{5/4} \bar{L}^{-4} \mu_0 \quad (0.19)$$

Model summary

The overall secondary nucleation rate considering both crystal-impeller and crystal-crystal collisions can now be found by substitution of the secondary nucleation rate equations of the individual processes in Eq. (2.2):

$$J_t = \Omega \cdot \left(K_{c-i} \cdot \left(\frac{K}{P_0} \right) \cdot \varepsilon \cdot k_v \cdot \rho_c \cdot \mu_3 + K_{c-c} \cdot \rho_{sl} \cdot x \cdot \varepsilon^{5/4} \cdot \bar{L}^{-4} \cdot \mu_0 \right), \quad (0.20)$$

where K_{c-i} and K_{c-c} are proportionality constants for crystal-impeller and crystal-crystal collisions respectively. The moments of distribution are given by:

$$\mu_3 = \int_{L_{c-i}}^{\infty} L^3 \cdot n_L \cdot dL,$$

and

$$\mu_0 = \int_{L_{c-c}}^{\infty} n_L \cdot dL$$

3. Experimental setup

To obtain the parameters of the kinetic framework two crystallizer configurations are used. In this section these configurations will be discussed briefly. The first configuration is a Draft Tube (DT) crystallizer with an operating volume of 22 litres. It is an evaporator-type DT agitated crystallizer, which can be operated in a fed-batch as well as in a continuous mode. This crystallizer is illustrated in Fig. (3.1.a). The crystallizer body is a cylindrical vessel with a height of 1 m and an internal diameter of 0.23 m with a flat head and a contour-shaped base. The nominal volume is

approximately 22 litres. The crystallizer is fitted with a draft tube (height 0.5 m, internal diameter 0.15 m, and outer diameter 0.17 m) that consists of two segments. The lower segment is a spirally baffled jacket heat exchanger through which hot water is pumped to supply the heat for evaporation of the solvent. The upper segment is made of solid stainless steel. A three-bladed marine-type impeller with a diameter of 0.14 m is used to pump the suspension through the draft tube upwards to the boiling zone. The impeller frequency can be varied up to 1400 rpm and the corresponding attainable superficial fluid velocity is 1.3 m/s. The vessel and draft tube are fitted with vertical baffles to reduce the impeller-induced rotational momentum by diverting it to the axial direction.

Table 3.1: Default operating conditions for both crystallizer types

	DT	DTB
Crystallizer volume [l]	22	1100
Temperature [°C]		50
Specific heat input [kW/m ³]		120
Feed temperature [°C]		53
Feed density [kg/m ³]		1248
Residence time [s]		4500
Product removal flow [l/s]	$4.88 \cdot 10^{-3}$	$2.44 \cdot 10^{-1}$
Fines removal flow rate [l/s]	-	2
Volume for fines dissolution [l]	-	240

The second crystallizer is a Draft tube baffled (DTB) evaporative crystallizer, which is given in Fig. (3.1.b) and that can be operated either in a fed-batch or a continuous mode. Crystallizer body is a cylindrical vessel with a dished head and a contoured-shaped base. The body has a total height of 4 m and an outer diameter of 0.7 m. The effective volume is estimated to be 1100 litre. The lower part of the crystallizer body is surrounded by an annular zone with a height of 1.5 m, an outer diameter of 1.2 m and a total volume of approximately 775 litre. The hull that separates the annular zone from the crystallizer body is the so-called skirt baffle. The crystallizer body is equipped with a draft tube with a height of 2.3 m and a diameter of 0.5 m. A marine-type impeller with a diameter of 0.485 m is used to circulate the contents of the crystallizer through the draft tube upwards to the boiling zone. The maximum impeller frequency is 370 rpm, which corresponds to a superficial velocity of 1.1 m/s. The annular zone surrounding the crystallizer body has a cross-sectional area of 0.746 m². Large baffles divide this zone across the entire height into six equally spaced, independent compartments. From the top of each compartment a so-called fines flow is removed via a withdrawal tube. The bottom of each compartment has an open connection to the crystallizer body. The relatively large cross-sectional area in combination with a low fines removal rate (up to 3.5 l/s) leads to a low vertical upward velocity inside the compartments. Due to this low velocity the annular zone will act as settling zone in which small crystals are separated from larger crystals by gravitational forces. Larger crystals will subsequently return to the crystallizer body

whereas small crystals are removed with the fines flow. In industrial processes, the DTB-crystallizer is employed to obtain larger average crystal sizes and narrower size distributions than can be produced in a DT-crystallizer. The default operating conditions for both crystallizers is given in Tab. (1). The used experiments, which only differ in impeller frequency are summarized in Tab. (2).

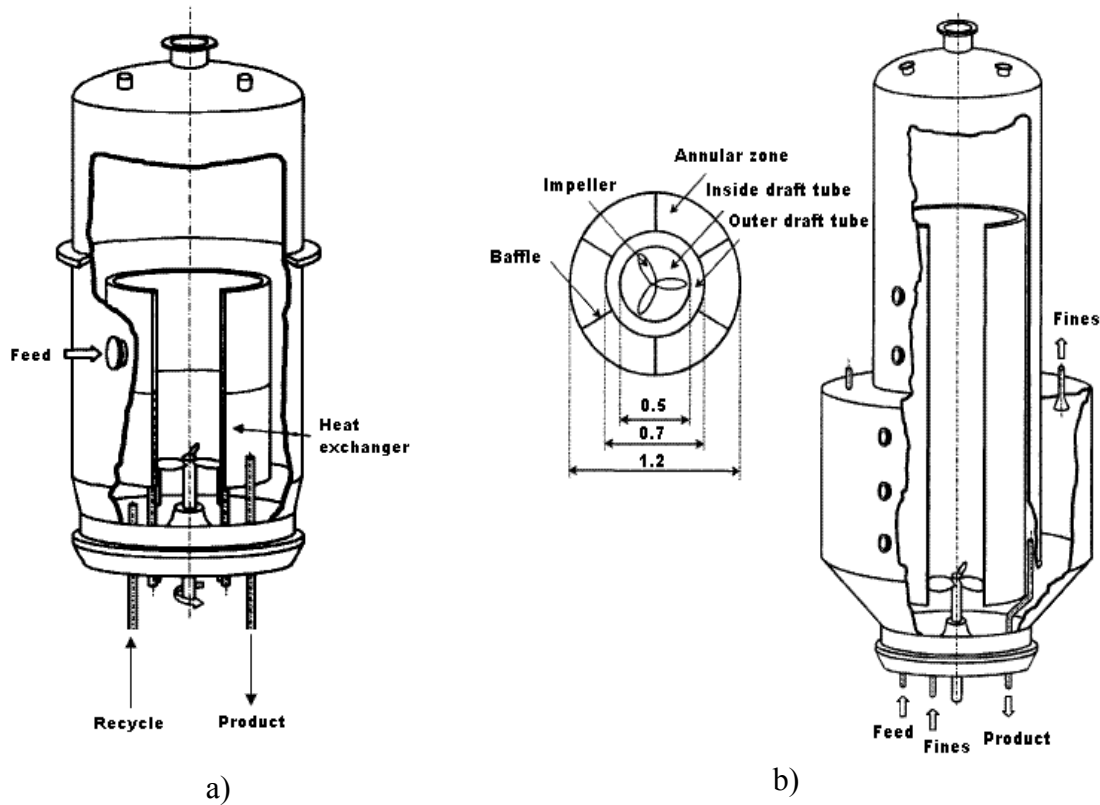


Figure 3.1: a) Schematic view of a 22L DT evaporative crystallizer and b) a 1100L DTB evaporative crystallizer

4. Results and discussion

Two crystallizer types, a 22-liter Draft Tube (DT) crystallizer and an 1100-liter Draft Tube Baffled (DTB) crystallizer are used which differ both in scale and configuration, to investigate the effect of the impeller frequency and the effect of scale on the CSD. The DT25-experiment is used in order to estimate the parameters of the kinetic framework. The estimation is done using the built-in parameter estimation routine that is available in gPROMS. It should be noted that the first four to five hours of experimental data are not used in the parameter estimation due to the fact that in these first four to five hours, the primary nucleation is dominant and the kinetic model is only based on secondary nucleation. During the start-up phase of the crystallization experiments two nucleation mechanisms are involved: primary and secondary nucleation. As the experiment progresses and crystal growth produces crystals sufficiently large to be prone to attrition, secondary nucleation becomes the dominant

mechanism. After this time, equal to approximately three to four residence times, it is expected that no primary nuclei will be present in the crystallizer. The basic assumption is that besides nucleation and growth no other physical processes (e.g. agglomeration, breakage) are considered. The growth rate is described with first order diffusion and second order surface integration.

The measured and simulated CSD's are presented in Fig. 4.1. Clearly a high quality fit is obtained in which both the steady-state crystal size and the CSD-dynamics are very good described. The parameters estimated using DT25 experiment will be used to describe the CSD in other DT-crystallizer experiment.

Table 4.1: Used experiments and corresponding impeller frequencies

Exp.	N [rpm]	Exp.	N [rpm]
DT19	550	DT26	910
DT22	640	DTB12	320
DT25	775	DTB03	370

The developed model contains seven parameters out of which four parameters were found to be reasonable constant at the different process conditions and are therefore

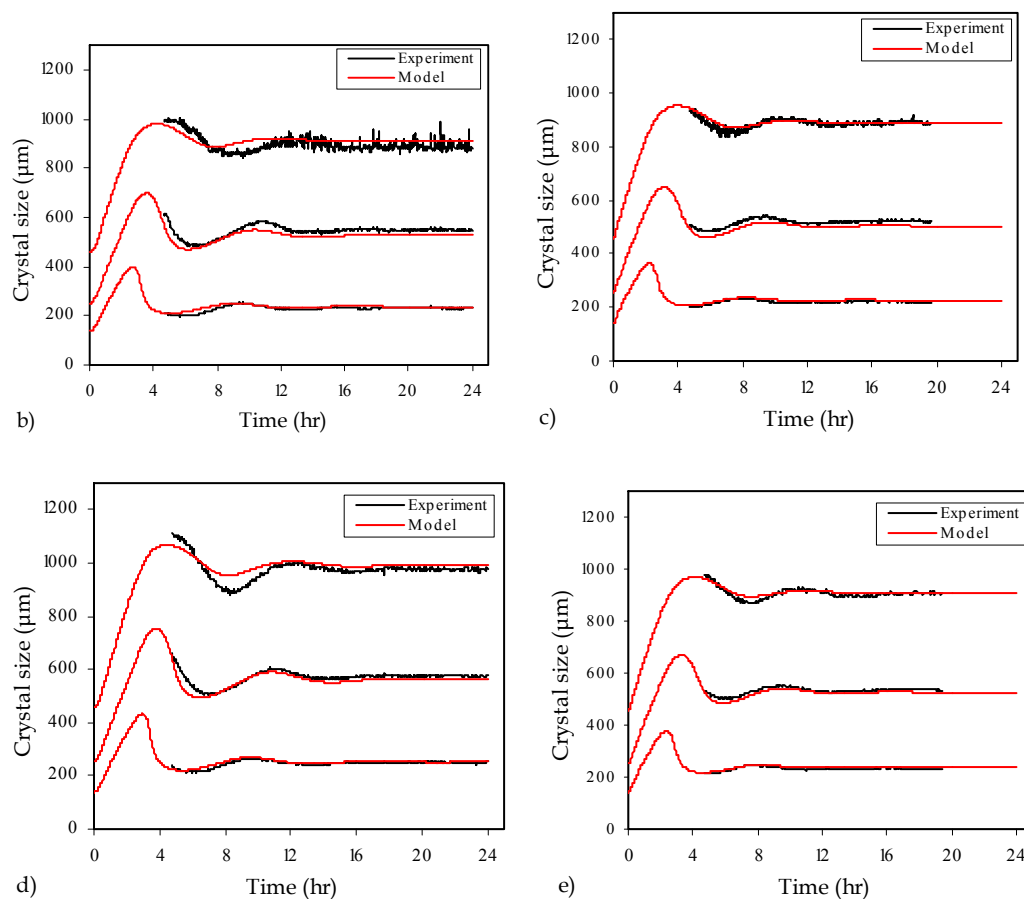


Figure 4.1: Measurements versus model predictions of quantiles L_{10} , L_{50} and L_{90} for experiment a) DT19, 550 rpm; b) DT22, 640 rpm; c) DT25, 775 rpm and d) DT26, 910 rpm.

considered to be system dependent. Three of the model parameters, the number of nuclei per unit energy (Ω), the lower bound of integration for crystal-impeller and for crystal-crystal collisions are considered to be system as well as process dependent and

found to be the function of impeller frequency. A correlation was found between the impeller speed and the model parameter that describes the Ω . An almost parallel linear fit on log-normal scale is found for Ω in the 22L DT crystallizer (Figure 4.2). A possible explanation for this relation is given by Neumann (2001). He showed, using SEM pictures, that due to an increase in power input (or impeller frequency) the corners of the

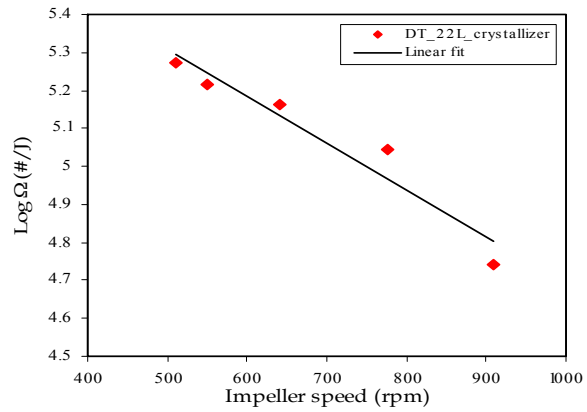


Figure 4.2: Parameter Ω plotted against the impeller speed

crystal become increasingly rounded-off. This is attributed to the fact that there is insufficient time between two successive attrition events experienced by a crystal corner to allow healing. In the approach by Gahn it is assumed that attrition takes place after the corners of a crystal are completely healed. If the impeller frequency increases, healing is no longer complete and the number of produced nuclei and consequently the efficiency of nuclei production is reduced. An alternative explanation for this phenomenon could be that the Ω is supersaturation dependent as suggested by Evans (1974). In our simulations Ω is assumed to be constant over the whole simulation.

It was found that in the 22-liter DT-crystallizer crystal-impeller collisions are dominating while crystal-crystal collisions are of less importance. Nevertheless, crystal-crystal collisions cannot be neglected and are especially pronounced at low impeller frequencies.

To look at the scale up capacity of the model, it is applied on the 1100L DTB crystallizer. The measured and predicted CSD for DTB-crystallizer, the experiments DTB03 and DTB12 are presented in Fig. 4.3. As can be seen, the simulation for DTB03 shows a high quality fit with the experimental data. For the experiment where the solution is agitated at 320 rpm (DTB12), the L_{90} is not plotted, since the experimental data was not accurate. In the 1100-liter DTB-crystallizer the term of the secondary nucleation rate equation describing crystal-crystal collisions seems to be more important. This effect cannot be attributed only to crystal-crystal collisions, but suggest the existence of a different secondary nucleation mechanism. Since the supersaturation in the DTB-crystallizer is higher and the circulation time is larger compared to the DT-crystallizer, it is expected that also the surface breeding could occur in this crystallizer. Dedicated experiments are discussed to validate this hypothesis.

5. Conclusions

The secondary nucleation model considering both crystal-impeller and crystal-crystal collisions looks very promising. Despite the fact that the model is relatively simple it gives very good description of the CSD with high accuracy. Both the dynamics of the CSD and the steady-state crystal size are described correctly. Even when a difference in scale and configuration is introduced, the obtained CSD is still very good.

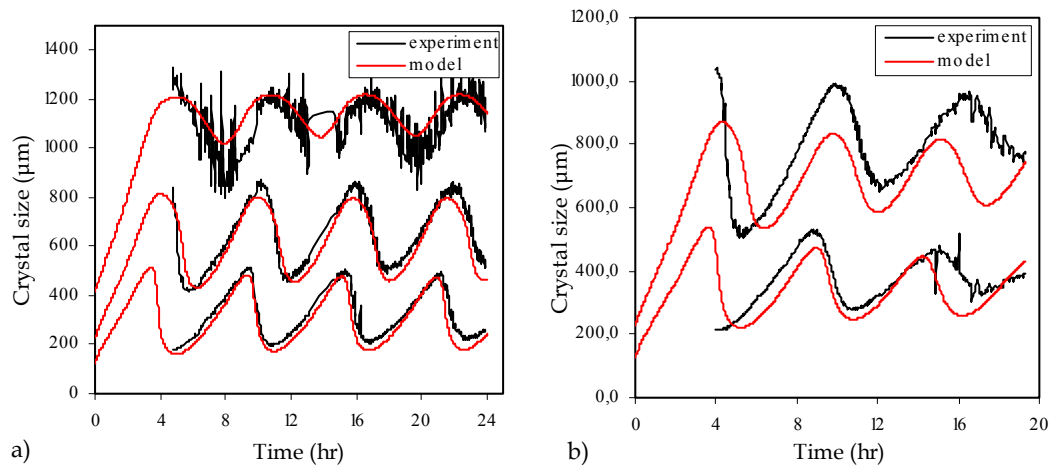


Figure 4.3: Measurements versus model predictions of quantiles L_{10} , L_{50} and L_{90} for the (a) DTB03 experiment. (b) DTB12 experiment

Three parameters of the model, number of nuclei per unit driving force, Ω , the lower bound of integration for crystal-impeller collisions and the lower bound of integration for crystal-crystal collisions are found to be system as well as process dependent and are a function of the impeller frequency. The number of nuclei per unit driving force is a linear function (on log-normal) scale of the impeller frequency. This is attributed to the time available for healing of the crystal corners between two subsequent collisions with the impeller. Due to small circulation time, healing time is relatively short, resulting in more rounded crystals. The overall effect is that an increase in impeller frequency results in a decrease in the number of nuclei generated.

Description of the initial part of the CSD is less accurate especially for higher impeller frequencies in the DT-experiments. This is due to the fact that the parameters of the initial distribution are estimated from the DT-25 experiment and are assumed to be constant for each experiment. The implementation of a primary nucleation model or the re-estimation of the distribution parameters are the possible solutions to get a better description of start up behavior and should be investigated. An important step in the approach towards a more scale independent model could be the extension of the secondary nucleation model by a third term, which describes the surface breeding.

6. References

Contribution of crystal-impeller and crystal-crystal collisions to secondary nucleation

- 1 Bermingham S.K., *A design procedure and predictive models for solution crystallization processes*, Delft University of technology, the Netherlands (2003).
- 2 Clontz N.A., and McCabe W.L., *Contact nucleation of magnesium sulphate heptahydrate*, Symposium. Series. AIChE (1971).
- 3 Daudey P.J., *Crystallization of ammonium sulphate – secondary nucleation and growth kinetics in suspension*, Delft University of technology, the Netherlands (1987).
- 4 Evans T., Margolis G., Sarofim A. F., *Mechanisms of secondary nucleation in agitated crystallizers*, AIChE Journal, (1974).
- 5 Evans T., Margolis G., Sarofim A. F., *Models of secondary nucleation attributable to crystal-crystallizer and crystal-crystal collisions*, AIChE Journal (1974).
- 6 Gahn C., and Mersmann A., *Theoretical Prediction and Experimental Determination of attrition rates*, Trans. Inst. Chem. Eng. (1997).
- 7 Gahn C., Mersmann A., *Brittle fracture in crystallization processes part B. Growth of fragments and scale-up of suspension crystallizers*, Chemical Engineering Science (1999).
- 8 Kramer, H.J.M., Rosmalen van., G. M., *Crystallization*, Delft University of technology, The Netherlands (2000).
- 9 Levich, V.G., *Physicochemical Hydrodynamics*, Prentice-Hall Inc., New Jersey (1962).
- 10 Ma, D.L., Tafti, D.K., and Braatz, R.D., *Optimal control and simulation of multidimensional crystallization Processes*, Computational Chemical Engineering (2002).
- 11 Menon A, *A task based design procedure and modeling approaches for industrial crystallization processes*, Delft University of technology, The Netherlands (2006).
- 12 Mersmann, A., *Crystallization technology handbook*, Dekker, New York (1995).
- 13 Mersmann A., *Supersaturation and nucleation*, Trans. Inst. Chem. Eng. A., (1996).
- 14 Mullin J.W., *Crystallization, third edition*, Butterworth-Heinemann, Oxford (1993).
- 15 Neumann A, *Characterizing industrial crystallizers of different scale and type*, Delft University of technology (2001).

- 16 Ó Meadhra R., *Modelling of the kinetics of Suspension Crystallizers; a new model for secondary nucleation*, Delft University of technology, the Netherlands (1995).
- 17 Ottens E. P. K., Janse, A. H., de Jong E. J., *Secondary nucleation in a stirred vessel cooling crystallizer*, Journal of Crystal Growth (1972).
- 18 Ottens E. P. K., de Jong E. J., *A model for secondary nucleation in a stirred vessel cooling crystallizer*, Industrial Engineering chemistry Fundamentals (1973).
- 19 Perry J.H., *Chemical engineers' handbook*, McGraw-hill book company, New York, third edition (1950).
- 20 Van Beusichem R., *Secondary nucleation attributable to the combine effects of crystal-impeller and crystal-crystal collisions*, graduation thesis, Delft University of technology (2006).
- 21 Virone C., *A fundamental approach to crystal growth and sono-crystallization*, Delft University of technology, the Netherlands (2006).
- 22 Westhoff, G.M., *Design and analysis of suspension crystallizers, aspect of crystallization kinetics and product quality*, Delft University of technology, the Netherlands (2002).
- 23 Wolf E., *Modelling the behaviour of solution crystallization processes for different scales and configurations*, Graduation thesis, Delft University of technology, the Netherlands (2007).